analytical chemistry

Article

pubs.acs.org/ac

Microfluidic Capillaric Circuit for Rapid and Facile Bacteria Detection

Ayokunle Oluwafemi Olanrewaju, Andy Ng, Philippe DeCorwin-Martin, Alessandra Robillard,† and David Juncker*

Biomedical Engineering Department, McGill University, 3775 rue University, Montreal, QC, H3A 2B4, Canada

Genome Quebec and McGill University Innovation Centre, McGill University, 740 Dr Penfield Avenue, Montreal, QC, H3A 0G1, Canada

Supporting Information

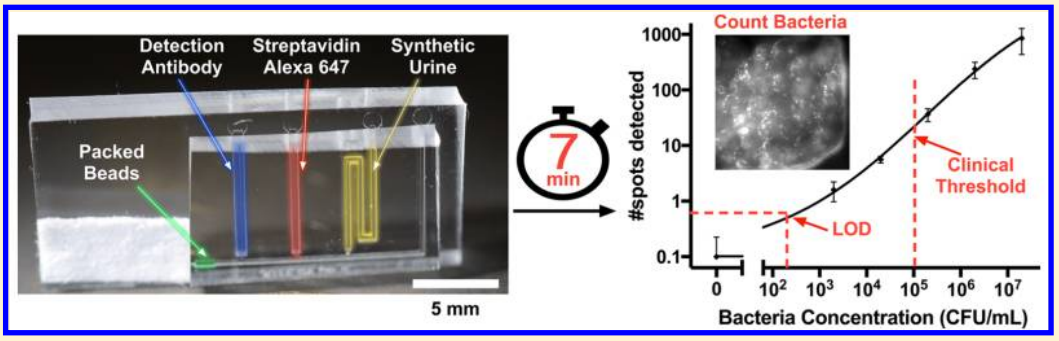

ABSTRACT: Urinary tract infections (UTI) are one of the most common bacterial infections and would greatly benefit from a rapid point-of-care diagnostic test. Although significant progress has been made in developing microfluidic systems for nucleic acid and whole bacteria immunoassay tests, their practical application is limited by complex protocols, bulky peripherals, and slow operation. Here we present a microfluidic capillaric circuit (CC) optimized for rapid and automated detection of bacteria in urine. Molds for CCs were constructed using previously established design rules, then 3D-printed and replicated into poly(dimethylsiloxane). CCs autonomously and sequentially performed all liquid delivery steps required for the assay. For efficient bacteria capture, on-the-spot packing of antibody-functionalized microbeads was completed in <20 s followed by autonomous sequential delivery of 100 μL of bacteria sample, biotinylated detection antibodies, fluorescent streptavidin conjugate, and wash buffer for a total volume ≈115 μL. The assay was completed in <7 min. Fluorescence images of the microbead column revealed captured bacteria as bright spots that were easily counted manually or using an automated script for user-independent assay readout. The limit of detection of *E. coli* in synthetic urine was 1.2×10^2 colony-forming-units per mL (CFU/mL), which is well below the clinical diagnostic criterion (>10^5 CFU/mL) for UTI. The self-powered, peripheral-free CC presented here has potential for use in rapid point-of-care UTI screening.

Up to 50% of women will get a urinary tract infection (UTI) by age 32.[1] UTI is caused by the presence of bacteria in urine, with over 80% of cases caused by *E. coli*.[2] The gold standard for detecting bacteria in urine is plate culture and the traditional clinical diagnostic threshold is ≥10^5 colony-forming units per mL (CFU/mL).[2,3] However, plate culture is slow (24−72 h to provide results), labor intensive, and centralized. Although dipstick tests are sometimes used in doctors' offices for rapid UTI detection, they are indirect tests that detect nitrites and leukocytes, symptoms that might be indicative of infection, rather than the bacterial pathogens themselves; thus, dipsticks have low specificity and sensitivity.[4] Another approach for bacteria diagnosis in clinical microbiology laboratories is real-time PCR from urine samples.[5] However, conventional PCR requires extensive sample preparation to purify nucleic acids and bulky equipment for nucleic acid amplification.

Microfluidic devices offer the promise of rapid, miniaturized, and automated biochemical assays.[6,7] The use of microfluidic devices for detection of bacteria in urine has been recently reviewed.[8,9] Many microfluidic devices for bacteria detection aim to miniaturize and automate nucleic acid detection methods. For example, paper-based devices for integrated nucleic acid extraction, isothermal amplification, and visual detection were developed.[10,11] Yet nucleic-acid based detection methods require sample preparation steps including cell lysis and nucleic acid purification. These steps slow down the bacteria detection assay and increase test complexity, challenging integration, and automation at the point of care. Recently, DNA-based bacteria detection was accelerated by skipping the sample preparation and DNA amplification processes. Lam et al. developed a test with on-chip electrical bacterial lysis followed by electrochemical detection in <30 min.[12] Nevertheless, for rapid screening at a doctor's office or

Received: April 8, 2017
Accepted: May 25, 2017
Published: May 25, 2017

DOI: 10.1021/acs.analchem.7b01315
Anal. Chem. 2017, 89, 6846−6853

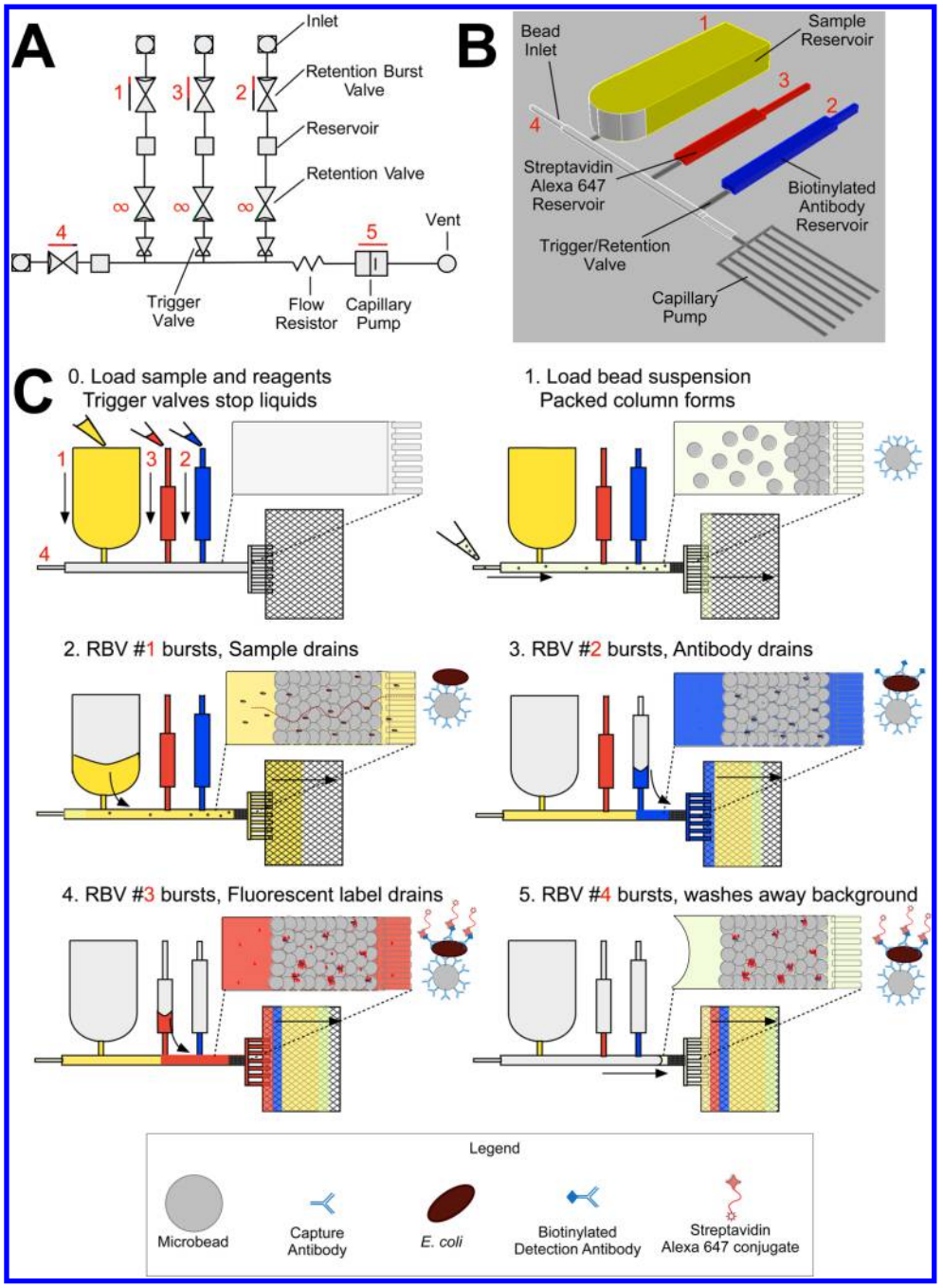

Figure 1. Design and working principle of CC for bacteria detection. (A) Symbolic layout showing modular design with individual capillaric fluidic elements.[23,24] (B) 3D schematic of CC showing the relative physical dimensions of various fluidic elements. (C) The assay is completed in 4 pipetting steps (C0) and 5 autonomous liquid delivery steps (C1−C5). Insets show close-ups of the packed bead column and individual assay steps on the bead surface (not to scale).

patient's home, it is desirable to further reduce both the test time and complexity.

Immunoassays that target whole bacterial cells using affinity binders such as antibodies enable bacteria detection without cell lysis.[13] Sandwich immunoassays, commonly used for specific protein detection, can be adapted to whole bacteria detection and even implemented in a multiplexed microarray format.[14,15] The availability of multiple bacterial extracellular receptors allows sensitive and specific capture of whole cells in immunoassays. However, the typical planar configuration of microfluidic immunoassays requires bacterial cells to diffuse to the sensing surface, which is slow given the relatively large size and low diffusivity of bacterial cells.[16] Consequently, to reduce assay time immunoaffinity columns consisting of packed microbeads functionalized with antibodies are used to provide large and distributed areas for bacterial capture.[17−21] The reported limit of detection in immunoaffinity columns for bacteria capture is as low as 10^4 CFU/mL,[18] thus meeting the diagnostic requirement for UTI.

However, bacteria capture with packed beads typically uses peripheral equipment such as syringe pumps for bead packing and subsequent sample and reagent delivery. To enable point-of-care immunoaffinity columns for rapid bacteria capture, there is a need for minimally instrumented and user-friendly

DOI: 10.1021/acs.analchem.7b01315
Anal. Chem. 2017, 89, 6846−6853

liquid handling in microfluidic devices. Autonomous capillary microfluidic systems are an attractive platform for minimally instrumented and self-powered immunoassays.[22] Our lab developed capillaric circuits (CCs) for preprogrammed and self-powered delivery of multiple liquids.[23] More recently, we presented analytical and empirical design rules for CCs manufactured by rapid prototyping of molds with a benchtop 3D-printer.[24] Here we optimize and apply CCs for rapid and facile detection of bacteria that requires only four pipetting steps and performs five functional steps. Preassembled microbead columns are not compatible with capillary flow as they can lead to bubble entrapment. Thus, we introduce on-the-spot assembly of microbead columns in CCs, followed by autonomous and sequential delivery of bacteria sample and sandwich immunoassay reagents in <7 min. Captured bacteria are detected using biotinylated antibodies and fluorescent streptavidin conjugates with fluorescence results that are easily interpreted by the user or an automated image analysis algorithm.

DESIGN AND WORKING PRINCIPLE OF CAPILLARIC CIRCUIT

Our goal was to develop a self-powered microfluidic device for rapid and simple detection of bacteria. To accomplish this, we integrated a microbead column within the CC to increase the surface area available for bacteria detection while simultaneously ensuring contact of bacteria to the surface, thereby improving detection sensitivity.

On the basis of our previous work,[24] a CC with a constriction to assemble a microbead column and 4 sequential retention burst valves (RBVs) was designed to capture and detect bacteria. The design of the modular CC was optimized and guided using a combination of symbolic (Figure 1A) and schematic layouts (Figure 1B).

Operation of the CC for bacteria detection is illustrated in Figure 1C. An assay is prepared by first preloading the sample and the two assay reagents to their respective inlets thereby filling the reservoirs. Preloading sample and reagent reservoirs is a preparatory step that can be completed up to 30 min before the start of the assay and in any order since liquids are held in place by capillary trigger valves (Figure 1C0).[24]

The preprogrammed assay is then initiated by the fourth pipetting step, which is loading the buffer containing beads. This triggers the automated five steps required for the bacteria capture assay in the CC without need for further user intervention. First, microbeads are assembled on-the-spot in the microchannel at a physical barrier (Figure 1C1) immediately followed by bacteria sample which is flowed through the microbead column resulting in the capture of whole bacterial cells by antibodies on the microbead surface (Figure 1C2). Next, biotinylated detection antibodies are flowed through the microbead column and bind to captured bacteria (Figure 1C3), followed by fluorescent streptavidin Alexa 647 conjugate which binds to biotinylated detection antibodies (Figure 1C4). Finally, wash buffer, which is comprised of the residual buffer from step no. 1, is flowed through the microbead column to remove unbound streptavidin (Figure 1C5).

Design of Microbead Column. The microbead column is a crucial component that influences the detection limit of this bacteria capture assay. There are several factors that affect bacteria capture in a microbead column including bacteria size, microbead size, sample volume, and sample flow rate. In the absence of accurate mathematical models that describe the influence of all these parameters, we empirically designed the microbead column for bacteria capture, in line with past work.[17−21]

Trapping microbeads with a physical constriction that is smaller than the microbead diameter is a simple and reliable way to pack beads in a microchannel.[17−20] The minimum feature size of the 3D-printer used to make the mold was a 50 μm vertical step,[24] which sets a lower limit on the size of microbeads that can be used. Although the keystone effect can be used to pack beads with a constriction that is larger than the microbead diameter,[25] it is sensitive to surface roughness (greater in 3D-printed channels than microfabricated ones) and requires a high temperature (115 °C) stabilization step to securely trap beads at the constriction. Thus, beads with a diameter ≥50 μm were used to ensure predictable and reliable bead packing at a 50 μm deep channel forming the constriction.

EXPERIMENTAL SECTION

Device molds were 3D-printed (Figure 2A) and replicated into PDMS (Figure 2B) as described in our past work.[24] Subsequently, the CC was evaluated in three steps: (i) verify preprogrammed liquid delivery operations using aqueous food dye solutions, (ii) validate basic assay operation and specificity by comparing capture of *E. coli* O157:H7 and K12 serving as positive and negative control, respectively, and (iii) determine limit of detection using serial dilution experiments with *E. coli* O157:H7 spiked into synthetic urine.

Verifying Preprogrammed Liquid Delivery. To test liquid delivery, the PDMS CCs were plasma-treated for hydrophilicity and sealed with flat hydrophobic PDMS covers prior to use. Aqueous food dye solutions were loaded in the reservoirs and the preprogrammed liquid delivery verified.[24] To characterize the reproducibility of bead packing and liquid delivery, five PDMS replicas from five different 3D-printed molds were tested with aqueous food dye solutions. Microbead column lengths and drainage times for each reservoir were recorded.

Validating Assay Operation and Specificity. *E. coli* O157:H7 ATCC strain 700728 (ATCC) was used as the model organism in our bacteria capture experiments. Synthetic urine (Surine Negative Control, DynaTek) with constituents that mimic human urine was used in on-chip experiments. Preactivated Ultralink bis-acrylamide/azlactone copolymer beads (ThermoFisher Scientific) were used for bacteria capture. Beads were functionalized with 10 μg/mL of anti-*E. coli* O157:H7 antibodies (BacTrace 01-95-90-MG, KPL) following the microbead manufacturer's specifications. Biotinylated anti-*E. coli* O157:H7 antibodies (BacTrace 16-95-90, KPL), and Streptavidin-Alexa Fluor 647 conjugate (S21374, ThermoFisher Scientific) were used to label and detect bacteria during the sandwich immunoassay. Reagents were diluted in 1× phosphate buffered saline (1× PBS, ThermoFisher Scientific).

To validate the general principle of the assay and determine its specificity, 10^6 CFU/mL each of *E. coli* K12 and *E. coli* O157:H7 was run through a CC containing beads and reagents that target *E. coli* O157:H7. A laboratory strain of *E. coli* K12, which lacks the O157 antigen, was generously provided by the Tufenkji lab at McGill University. Spots were counted manually.

Serial Dilution Experiments. We carried out the bacteria capture assay using synthetic urine spiked with *E. coli* O157:H7. *E. coli* O157:H7 samples were grown overnight in LB medium

DOI: 10.1021/acs.analchem.7b01315
Anal. Chem. 2017, 89, 6846−6853

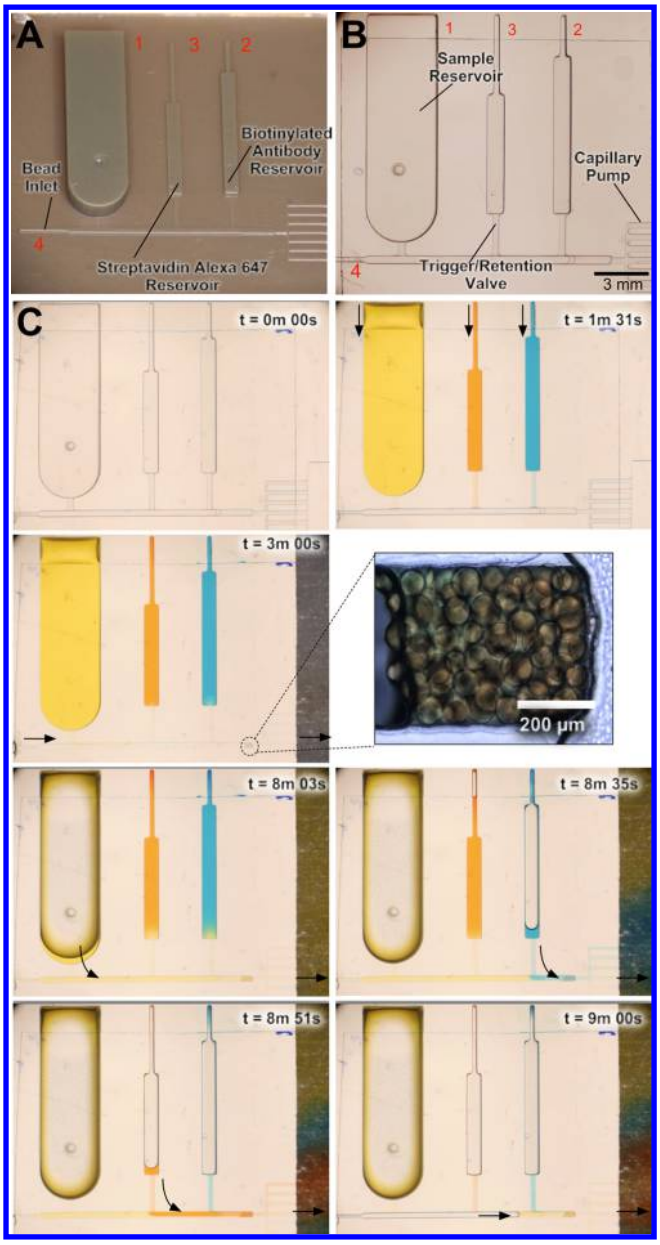

Figure 2. Fabrication and testing of CC for bacteria detection. (A) 3D-printed mold of the CC. (B) Final CC replicated into PDMS. (C) Time-lapse images of preprogrammed liquid delivery in CC. Arrows indicate flow direction. See Movie S1.

at 37 °C. Subsequently, serial dilutions of bacteria suspension were prepared in synthetic urine. Samples with bacterial concentrations of 0, 10^3, 10^4, 10^5, 10^6, and 10^7 CFU/mL were prepared. Bacteria serial dilutions were plated on LB agar culture plates at room temperature for 24 h to count and confirm the number of bacteria present in each sample. Subsequently, bacteria suspensions were used for on-chip experiments to characterize bacteria capture in CCs. To determine the sensitivity of the assay, a binding curve was established by plotting the number of spots observed in the microbead column with the known bacterial count from plate culture.

Bacteria Counts and Calculation of Limit of Detection. After completion of the assay in the CC, the microbead column was imaged at 20× magnification using an inverted fluorescence microscope (TE-2000-E inverted microscope, Nikon) equipped with a CCD camera (QuantEM 512SC, Photometrics). Manual counts of the number of bacteria in each bead column were carried out by 5 volunteers blinded to the true test results. One labeled image with 5 spots (10^4 image in Figure 4A) was presented as a training image to the volunteers who were instructed to identify similar spots in all other images. All images, including the negative controls, were presented in a random order. At higher concentrations (i.e., 10^5, 10^6, 10^7 CFU/mL), the number of spots was estimated by counting the number of spots in a quarter of the bead column and multiplying by 4. This is similar to the colony counting technique employed in standard microbiology. Spot counts from the 5 volunteers were averaged for each image. Subsequently, average spots counts were obtained for each bacteria concentration using images from 3 different CCs.

All experiments were performed in triplicate unless otherwise stated. The data from manual bacteria counts was fitted with a nonlinear four-parameter logistic curve using GraphPad Prism 7 (GraphPad Software Inc., La Jolla, CA). The limit of detection (LOD) was calculated using the 3-sigma criterion, i.e., finding the intersection of the blank plus 3 times the standard deviation of the blank with the nonlinear curve fit. Similarly, the limit of quantification was calculated using the 10-sigma criterion.

Algorithm for Automated Bacteria Counts. To provide automated bacteria counts, a MATLAB script was written to analyze assay images. The image analysis algorithm is provided in the Supporting Information. First, images were manually cropped to remove the edges of the bead column since they create artifacts in subsequent image processing steps. Next, a Gaussian filter was applied to normalize images. At 20× magnification, 1 pixel in each fluorescence micrograph corresponded to 2 μm in size. Given that *E. coli* are expected to be ≈2 μm × 1 μm, we expected bacteria to appear as ≈4-pixel diameter "spots" in the fluorescence micrographs. Consequently, spots were identified using an opening top-hat filter with a disk radius of 2 pixels and a Laplacian of Gaussian filter to match the expected size of detected bacteria in the bead column. Both the top-hat and the Laplacian of a Gaussian filters identify bright point-like features in which the 2-pixel radius disk can fit. An H-max transform was used to remove low regional peaks. A threshold was then applied based on the average signal of the image to form a black and white image.

In less than 20% of the captured images, larger spots (≈ 20–50 pixels in diameter) that appeared to come from dust or debris were splintered during the image thresholding step and counted as bacteria by the automated script. To avoid these spurious counts, an opening and closing by reconstruction operation was performed with a larger disk with a 5-pixel radius. By thresholding the resulting image, these large areas with bright fluorescence were ignored.

RESULTS AND DISCUSSION

A CC for rapid and facile bacteria detection was designed and tested. The cross-section and capillary pressure of each RBV required for preprogrammed liquid delivery in the CC is summarized in Table 1. Device molds were 3D-printed (Figure 2A) and replicated into PDMS (Figure 2B).[24] The sample reservoir (inlet 1) was designed to have a volume of 100 μL while retaining a compact footprint (2 × 4 × 13 mm^3) as seen in Figure 2B. Meanwhile, the biotinylated antibody reservoir (inlet 2) and streptavidin conjugate reservoir (inlet 3) had volumes of 4.7 μL and 2.4 μL, respectively. These volumes were empirically found to provide a good signal-to-noise ratio

DOI: 10.1021/acs.analchem.7b01315
Anal. Chem. 2017, 89, 6846–6853

Table 1. Geometry of Retention Burst Valves (RBVs) in CC for Detection of Bacteria[a]

	width (μm)	height (μm)	capillary pressure (Pa)
RBV1	4000	2000	−93
RBV2	300	500	−667
RBV3	300	300	−834
RBV4	200	250	−1126
capillary pump	200	50	−2602

[a]RBV heights and widths were designed to ensure sequential delivery of sample and assay reagents according to previously established design rules.[24]

for bacterial imaging. The central branch (inlet 4) had a volume of 1.4 μL and was used to introduce the microbead suspension to the circuit.

Preprogrammed Liquid Delivery in Capillaric Circuit. We verified sequential liquid delivery using aqueous food dye solutions (Figure 2C). A volume of 100 μL of liquid was added to the sample reservoir, 4.7 μL was added to the biotinylated antibody reservoir, and 2.4 μL was added to the Streptavidin-Alexa 647 reservoir (Figure 2C, t = 1 min 31 s). Trigger valves held the sample and reagents in place for at least 30 min allowing sufficient time to preload the chip and conveniently start the assay without worrying about the timing of the reagent loading steps.[23,24]

In the CC design, flow of the sample and assay reagents is triggered by adding the microbead solution to inlet 4. This initiates on-the-spot packing of microbeads in front of the capillary pump as the first step in the on-chip immunoassay. We added 7 μL containing a 1% w/v bead suspension in 1× PBS to inlet 4 (Figure 2C, t = 3 min 0 s). Adding the bead suspension to inlet 4 filled the central branch and connected all reservoirs in the CC to the capillary pump. At this point, the capillary pump and RBVs determined the sequence of liquid delivery without user intervention. The sample reservoir drained first since it had the lowest capillary pressure (Figure 2C, t = 8 min 3 s). It is noteworthy that the position of the RBVs relative to the capillary pump does not determine their drainage sequence; instead it is the capillary pressure of the microchannel (set by its geometry and surface chemistry) that controls the drainage sequence. Next, RBV2 burst and the biotinylated antibody reservoir drained (Figure 2C, t = 8 min 35 s), then RBV3 and the streptavidin Alexa 647 conjugate reservoir (Figure 2C, t = 8 min 51 s) and finally, RBV4 and the central branch (Figure 2C, t = 9 min 0 s). Laminar flow in the CC ensures that the remaining sample and wash buffer in the central channel effectively washed away the streptavidin Alexa 647 conjugate solution from the bead column thereby reducing background fluorescence. The total liquid delivery time since microbead addition was 6 min 0 s.

The packed microbead column may be imaged in real-time during the assay or afterward when the microchannels are dry. The microbeads were readily visible with a brightfield microscope and captured bacteria were readily visible with a fluorescence microscope.

Reproducibility of Bead Packing and Liquid Delivery. To determine the reproducibility of liquid delivery in the circuit, we tested five PDMS replicas from five different 3D-printed molds. This represents the worst case scenario in reproducibility of liquid delivery since replicas can be made from a single mold to minimize mold-to-mold variability that arises during manufacturing. We recorded bead column lengths and liquid delivery times after preprogrammed drainage was initiated by adding the bead suspension to inlet 4. Over five experiments, the average bead column length was 888 ± 144 μm. Meanwhile the average flow rates for the sample, biotinylated antibody, streptavidin Alexa 647 conjugate, and wash buffer were 0.36 ± 0.07, 0.23 ± 0.06, 0.21 ± 0.04, and 0.18 ± 0.05 μL/s, respectively. The average assay time over all five experiments was 5.5 ± 1.0 min. The coefficient of variation in liquid delivery times (18.7%) is consistent with observations in our previous work with 3D-printed CCs and is thought to arise primarily from variations in surface chemistry and handling of PDMS devices.[24]

Validating Assay Principle and Specificity. As a proof of principle test of assay sensitivity and specificity, 10^6 CFU/mL each of the target *E. coli* O157:H7 and nonpathogenic *E. coli* K12 were run through bacterial capture assays in CCs with microbeads functionalized with anti-*E. coli* O157:H7 capture antibodies and detection antibodies that also target *E. coli* O157:H7. When the sample was *E. coli* O157:H7, multiple spots (238.1 ± 62.5, N = 3) were observed in the microbead column (Figure 3). This test was a positive control showing that the overall principle of the sandwich immunoassay with spot counting was viable. In contrast, when the sample was 10^6 CFU/mL of *E. coli* K12, very few spots (5.7 ± 7.2, N = 3) were observed in the microbead column, demonstrating specificity of the sandwich immunoassay.

Limit of Detection of *E. coli* in Synthetic Urine. To determine the limit of detection of the bacteria capture assay, the following concentrations of *E. coli* O157:H7 were spiked

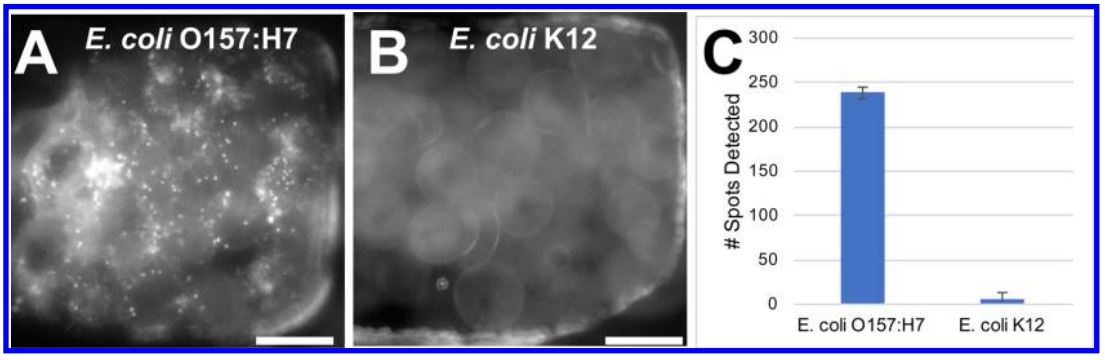

Figure 3. Validating assay principle and specificity by comparing bacteria capture after flowing 10^6 CFU/mL of *E. coli* O157:H7 and K12 through CCs designed for *E. coli* O157:H7 capture. (A) Multiple spots in bead column after flowing *E. coli* O157:H7. (B) Few spots in bead column after flowing *E. coli* K12. (C) Bar graph quantifying specific capture of *E. coli* O157:H7. Error bars indicate standard deviation. N = 3.

DOI: 10.1021/acs.analchem.7b01315
Anal. Chem. 2017, 89, 6846−6853

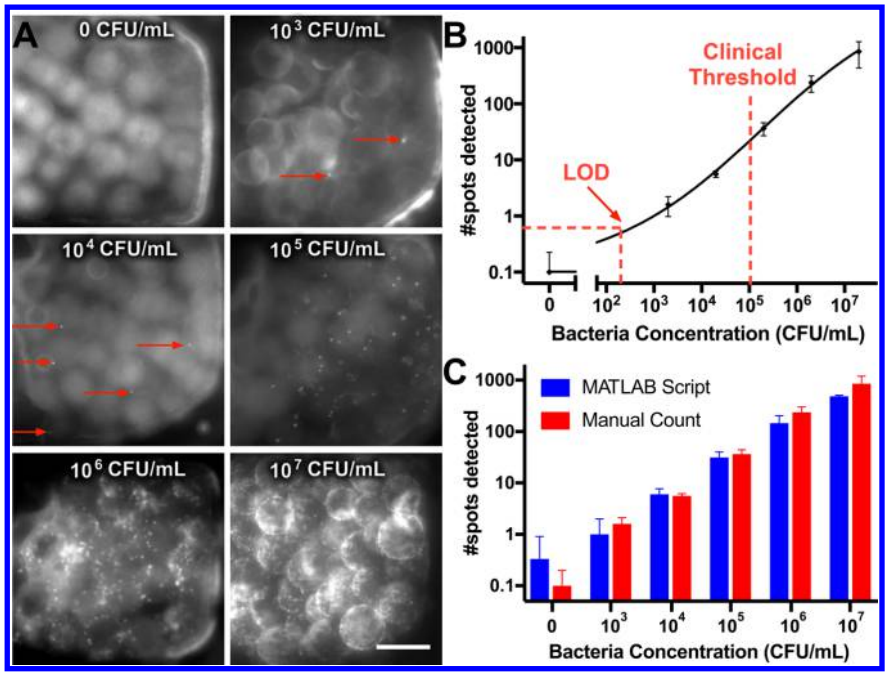

Figure 4. Results of bacteria capture assay in CC, standard curve for calculating limit of detection, and validation of automated script for bacteria counts. (A) Fluorescence micrographs showing captured bacteria in the microbead column of the CC. Scale bar is 100 μm. (B) log–log standard curve showing bacteria concentration versus no. of spots detected. The limit of detection (LOD) was 1.2×10^2 CFU/mL. $N = 3$. Error bars indicate 95% confidence intervals. (C) The MATLAB script provided similar results to manual counts performed by 5 individuals blinded to the true test results. Error bars indicate standard deviation. $N = 3$.

into synthetic urine and tested in the CC: 0, 10^3, 10^4, 10^5, 10^6, and 10^7 CFU/mL. Figure 4A shows raw data obtained from on-chip experiments. Captured bacteria were clearly visible as fluorescent spots that could be counted by the user. These "spots" were defined as bright fluorescence regions that are ≈2 μm in diameter when viewed with a 20× objective, since the target *E. coli* are ≈2 × 1 μm^2 in size. Such spots were easy to count in microscope images since they stood out from the background greyscale signal, as illustrated with arrows in Figure 4A. Residual fluorescence of antibodies on the beads was visible as halos that were readily distinguished from bacterial spots. The results shown in Figure 4A suggest that we could readily distinguish between low and high bacteria concentrations.

The number of spots detected at each bacteria concentration was plotted against the bacteria concentration determined by plate culture (the gold standard). Each bacterial sample was tested on 3 separate CCs. Spots were counted by 5 volunteers blinded to the true test results. Average spot counts were 0.1, 1.6, 5.6, 36.5, 238.1, and 854.9 spots at 0, 10^3, 10^4, 10^5, 10^6, and 10^7 CFU/mL, respectively. These results are displayed as a log–log curve in Figure 4B showing a steady increase in the number of spots detected as bacteria concentration increased.

The LOD was calculated using the 3-sigma criterion as 1.2×10^2 CFU/mL using a nonlinear four-parameter logistic curve fit of the log-transformed data. The limit of quantification was calculated using the 10-sigma criterion and was 1.5×10^3 CFU/mL. Both values are well below the traditional clinical threshold for bacteriuria (10^5 CFU/mL). Even though the calculated LOD was 1.2×10^2 CFU/mL, it is important to note that the lowest concentrations tested experimentally were 0 and 1×10^3 CFU/mL. Only two spots were observed at 1×10^3 CFU/mL (see Figure 4A). Consequently, a large number of experiments would be required to practically distinguish 1×10^2 CFU/mL from 0 CFU/mL. Nevertheless, the CC can readily distinguish between 1×10^3 CFU/mL and 0 CFU/mL meeting the conventional diagnostic threshold for UTI (1×10^5 CFU/mL). In addition, in Trade Off between Sensitivity and Time-to-Result, we describe strategies for improving the LOD of bacterial detection assay in the CC.

Algorithm for Automated Bacteria Counts. As described above, the number of bacteria captured in the CC can be readily counted by users with minimal training. To further facilitate ease of use at the point-of-care and to enable independent, quantitative, traceable, and comparable analysis, it is desirable to automate bacteria spot counting. As such, we developed a spot detection script using MATLAB.

To verify the bacteria counts by the automated algorithm, we compared the number of spots counted by the MATLAB algorithm with manual counts (Figure 4C). Good agreement was observed between the manual and automated bacteria counts with a few exceptions. The MATLAB script reported a higher average spot count for negative controls. Using the MATLAB script, individual spot counts of 0, 0, 1 were obtained the three images captured at 0 CFU/mL. Meanwhile, of the 5 individuals who performed blinded manual spot counts, all users reported no spots in the 0 CFU/mL images, except for one user who reported 1 spot in only 1 of the 3 negative control images. As a result, the average spot counts at 0 CFU/mL for the MATLAB algorithm and the manual counts were 0.33 ± 0.58 and 0.1 ± 0.1, respectively. Also, at higher concentration (>10^6 CFU/mL), there was a large (≈ 50%) difference between the manual and automated counts. This is because the background intensity levels of images differed significantly between the low and high concentration images, making it difficult to find a single thresholding algorithm that performs well over the 5 orders of magnitude of bacteria concentration tested in our experiments. This discrepancy at very high concentrations is not a major concern as primarily a

DOI: 10.1021/acs.analchem.7b01315
Anal. Chem. 2017, 89, 6846–6853

yes/no answer for bacteruria is sought with >10^5 CFU/mL as the cutoff. If quantitative measures are required at high concentrations, it should be possible to use other metrics such as the average image intensity. These results establish that automated analysis could be used for assay readout.

Trade-Off between Sensitivity and Time-to-Result. Although the CC for bacteria detection meets the traditional diagnostic requirement for bacteriuria (10^5 CFU/mL), recent reviews suggest that LODs as low as 10^2 CFU/mL may be required for some symptomatic patients with UTI, which is close to the LOD of our test.[2] The LOD of the CC may be further improved by 3D-printing CCs with finer features and using smaller microbeads to improve bacteria capture efficiency. As microbead diameter decreases, the bacteria capture efficiency increases[17,26] since the gap size between beads decreases and bacteria cells are more likely to contact the functionalized sensing surface. In this work, bead diameter was limited to sizes ≥50 μm-imposed by the resolution of the 3D-printer used. 3D-printers with minimum Z-feature sizes down to 10 μm have recently become available at a cost of ≈US $10 000, which is affordable for many research laboratories, and would allow trapping of much smaller beads.[27,28] However, given a constant capillary pressure, the flow resistance in the CC increases rapidly with smaller bead size and the time required to flow 100 μL of sample through the CC would increase significantly. The current CC design allowed processing of a large sample volume (i.e., 100 μL) in a short time with a capture efficiency of ≈1 in 100 bacteria. Applications that require bacteria detection at much lower concentrations could be addressed by using smaller beads, however, at the expense of much longer flow times. Hence, for each application optimization will be needed to identify the desired trade-off between capturing of sufficient bacterial particles while permitting sample processing within a given time.

Although patients with UTI typically produce spontaneous urine volumes of 20−200 mL which is significantly less than the volume produced by healthy individuals (100−550 mL),[29] we do not anticipate any problems related to small urine sample volumes. This is because the CC requires only a small aliquot (0.1 mL) of the patient sample to achieve clinically relevant sensitivity. In fact, we could increase the volume of urine sample screened to further improve the limit of detection of the assay. The sample volume screened could easily be doubled or tripled while keeping the same design and completing tests in <30 min, fitting within the typical duration of a doctor's office visit. Flow resistances in the CC could also be redesigned to process a larger sample volume while still providing results within the 7 min time frame shown here.

3D-Printing and Mass Production. 3D-printing was used for rapid and simple prototyping despite the size limitations imposed by the 3D printer (i.e., ≥ 200 μm lateral features and ≥50 μm vertical features). Also, 3D-printing provided the capability to easily fabricate millimeter-scale ($2 \times 4 \times 13$ mm^3) reservoirs to hold large (100 μL) sample volumes within the same device that contains micrometer-scale (200×50 μm^2) channels for capillary pumping. To implement mass production, the final mold design may be replicated into metal or directly manufactured by conventional means such as Computer Numerical Control (CNC) micromachining, followed by injection molding to produce many functional replicas. Alternatively, 3D-printing may be used as an initial step to generate silicone rubber molds for injection molding.[30,31] In future, advances in 3D-printing technology, such as 3D-printing of metals,[32,33] may provide sufficient resolution and smoothness for direct printing of metal molds for durable injection molding.

Ease of Use of the CC. Our aim was to develop a test that meets key criteria for use at the point-of-care, and we envision that the CC could be used by a medical practitioner (doctor, nurse, or technician) who would add liquids to on-chip reservoirs to start the test. Precise pipetting may not be required to operate the device and a disposable plastic liquid dropper could be used to fill reservoirs. Since trigger valves hold liquids in place, the chip could be designed to tolerate overfilling and excess liquids, which in the current design was simply wiped away from the inlets using a piece of paper, but which could be removed by overflow structures integrated into the CC.

Since the CC enables rapid, "walk-away" processing of samples, a user can set up multiple experiments in parallel. A series of CCs can be loaded with reagents over a period of 30 min, without worrying about precise timing of pipetting steps or removing liquids from the chip. All chips could then be triggered sequentially by adding different samples, and the result simply read out as soon as 7 min after the first chip was loaded, within 30 min or so to minimize the risk of postexperiment drying artifacts.

One can envision further improvements to make operation of the CC even simpler. For example, it may be possible to reduce the number of pipetting steps using a simpler design where antibodies and microbeads are spotted and dried on the CC, and only require rehydration with a buffer. This would allow development of a CC that only requires two steps, addition of wash buffer and addition of sample.

To facilitate inexpensive visual readout at the point-of-care, low-cost, and portable fluorescence microscopes[34,35] or cell phones with optical adaptors[36] may be used for quantitative, yet minimally instrumented detection. Similarly, chemical signal amplification may be used to provide colorimetric results that are visible to the naked eye.[37,38]

Compared to DNA-based tests and other non-nucleic acid bacteria detection tests, the primary advantage of our approach is the simplicity and speed achieved without sacrificing sensitivity. Most microfluidic-based approaches require external pumps and valves to automate each liquid handling step, making miniaturization and point-of-care use more challenging. In contrast, the CC automates sequential liquid delivery processes with minimal external equipment and without user intervention other than to start the assay.

■ CONCLUSION

In this paper, we demonstrate rapid and facile detection of bacteria in synthetic urine in <7 min using a self-powered and autonomous microfluidic CC with a LOD of 1.2×10^2 CFU/mL, which is well below the traditional clinical threshold for UTI detection (≥10^5 CFU/mL). The CC features on-the-spot packing of functionalized microbeads in <20 s which proved to be compatible with subsequent capillary-driven flow of sample and reagents. The CC is user-friendly as it only requires 4 pipetting steps to initiate the self-powered assay procedure and achieves clinically relevant results in a fraction of the time that it takes with competing technologies and without requiring bulky peripherals. The speed, simplicity, and sensitivity of the CC meets key requirements for use as a triage tool for screening patients suspected of having UTI. Rapid tests could allow

DOI: 10.1021/acs.analchem.7b01315
Anal. Chem. 2017, 89, 6846−6853

physicians to prescribe antibiotics only after confirmation of bacterial infection, thereby helping to reduce overprescription and minimize the emergence of antibiotic-resistant pathogens. Although *E. coli* causes 80−85% of UTI cases, other bacteria including *Klebsiella pneumonia* and *Staphylococcus saprophyticus* also regularly cause UTI.[2] By combining different affinity binders, CCs may be adapted to detect multiple pathogenic bacteria causing UTI. The CC will need to be validated using clinical urine samples to study the impact of matrix effects, patient-to-patient variation in urine properties, and the diversity of bacterial strains that cause UTI. Furthermore, the concept of CCs with packed microbeads should be suitable for other bacterial assays as well as for other analytes such as viruses or proteins.

■ ASSOCIATED CONTENT

Supporting Information

The Supporting Information is available free of charge on the ACS Publications website at DOI: 10.1021/acs.analchem.7b01315.

Video of liquid delivery in the capillaric circuit (see Figure 2C) (Movie S1), image analysis algorithm to automate bacteria spot counting (ZIP), and Computer-Aided Design file for Capillaric Circuit (ZIP).

■ AUTHOR INFORMATION

Corresponding Author

*E-mail: david.juncker@mcgill.ca.

ORCID

Ayokunle Oluwafemi Olanrewaju: 0000-0003-4776-1774

David Juncker: 0000-0002-7313-1162

Present Address

†A.R.: Sensoreal Inc., Montreal, QC, Canada.

Notes

The authors declare no competing financial interest.

■ ACKNOWLEDGMENTS

We thank NSERC and CIHR for funding. A.O.O. is grateful for funding from the NSERC CREATE Integrated Sensor Systems Training Program, the CIHR Systems Biology Training Program, and the Quebec Merit Scholarship for Foreign Students (PBEEE). D.J. acknowledges a Canada Research Chair. We are grateful for helpful discussions with Dr. Brian Ward, Dr. Nathalie Tufenkji, Arya Tavakoli, Sa Xiao, and Veronique Laforte at McGill University. We thank Edward Zhang, Eun Hae Oh, Maiwenn Beaugrand, Mcolisi Dlamini, Mohamed Yafia, and Rosalie Martel for their help with data analysis. A.O.O. thanks his McGill Graphos Peer Writing Group.

■ REFERENCES

(1) Hooton, T. M. *N. Engl. J. Med.* **2012**, *366*, 1028−1037.
(2) Foxman, B. *Nat. Rev. Urol.* **2010**, *7*, 653−660.
(3) Warren, J. W.; Abrutyn, E.; Hebel, J. R.; Johnson, J. R.; Schaeffer, A. J.; Stamm, W. E. *Clin. Infect. Dis.* **1999**, *29*, 745−758.
(4) Schmiemann, G.; Kniehl, E.; Gebhardt, K.; Matejczyk, M. M.; Hummers-Pradier, E. *Dtsch Arztebl Int.* **2010**, *107*, 361−367.
(5) Lehmann, L. E.; Hauser, S.; Malinka, T.; Klaschik, S.; Weber, S. U.; Schewe, J.-C.; Stüber, F.; Book, M. *PLoS One* **2011**, *6*, e17146.
(6) Whitesides, G. M. *Nature* **2006**, *442*, 368−373.
(7) Sackmann, E. K.; Fulton, A. L.; Beebe, D. J. *Nature* **2014**, *507*, 181−189.
(8) Mach, K. E.; Wong, P. K.; Liao, J. C. *Trends Pharmacol. Sci.* **2011**, *32*, 330−336.
(9) Kumar, M. S.; Ghosh, S.; Nayak, S.; Das, A. P. *Biosens. Bioelectron.* **2016**, *80*, 497−510.
(10) Choi, J. R.; Hu, J.; Tang, R.; Gong, Y.; Feng, S.; Ren, H.; Wen, T.; Li, X.; Wan Abas, W. A. B.; Pingguan-Murphy, B.; Xu, F. *Lab Chip* **2016**, *16*, 611−621.
(11) Lafleur, L. K.; et al. *Lab Chip* **2016**, *16*, 3777−3787.
(12) Lam, B.; Fang, Z.; Sargent, E. H.; Kelley, S. O. *Anal. Chem.* **2012**, *84*, 21−25.
(13) Shin, J. H.; Park, J.-K. *Anal. Chem.* **2016**, *88*, 10374−10378.
(14) Gehring, A. G.; Albin, D. M.; Bhunia, A. K.; Reed, S. A.; TU, S.-I.; Uknalis, J. *Anal. Chem.* **2006**, *78*, 6601−6607.
(15) Wolter, A.; Niessner, R.; Seidel, M. *Anal. Chem.* **2008**, *80*, 5854−5863.
(16) Squires, T. M. *Rev. Mod. Phys.* **2005**, *77*, 977−1026.
(17) Brewster, J. D. *J. Microbiol. Methods* **2003**, *55*, 287−293.
(18) Guan, X.; Zhang, H.-j.; Bi, Y.-n.; Zhang, L.; Hao, D.-l. *Biomed. Microdevices* **2010**, *12*, 683−691.
(19) Yoo, J. H.; Woo, D. H.; Chun, M.-S.; Chang, M.-S. *Sens. Actuators, B* **2014**, *191*, 211−218.
(20) Chang, M.-S.; Yoo, J. H.; Woo, D. H.; Chun, M.-S. *Analyst* **2015**, *140*, 7997−8006.
(21) Molloy, P.; Brydon, L.; Porter, A. J.; Harris, W. J. *J. Appl. Bacteriol.* **1995**, *78*, 359−365.
(22) Juncker, D.; Schmid, H.; Drechsler, U.; Wolf, H.; Wolf, M.; Michel, B.; de Rooij, N.; Delamarche, E. *Anal. Chem.* **2002**, *74*, 6139−6144.
(23) Safavieh, R.; Juncker, D. *Lab Chip* **2013**, *13*, 4180.
(24) Olanrewaju, A. O.; Robillard, A.; Dagher, M.; Juncker, D. *Lab Chip* **2016**, *16*, 3804−3814.
(25) Ceriotti, L.; De Rooij, N. F.; Verpoorte, E. *Anal. Chem.* **2002**, *74*, 639−647.
(26) Tufenkji, N. *Adv. Water Resour.* **2007**, *30*, 1455−1469.
(27) Au, A. K.; Huynh, W.; Horowitz, L. F.; Folch, A. *Angew. Chem., Int. Ed.* **2016**, *55*, 3862−3881.
(28) Waheed, S.; Cabot, J. M.; Macdonald, N. P.; Lewis, T.; Guijt, R. M.; Paull, B.; Breadmore, M. C. *Lab Chip* **2016**, *16*, 1993−2013.
(29) Truzzi, J. C. I.; Almeida, F. M. R.; Nunes, E. C.; Sadi, M. V. *J. Urol.* **2008**, *180*, 182−185.
(30) Mueller, T. Stereolithography-based prototyping: case histories of applications in product development. In *IEEE Technical Applications Conference and Workshops at Northcon/95*, Portland, OR, October 10−12, 1995; pp 305−310.
(31) Chung, P.; Heller, J. A.; Etemadi, M.; Ottoson, P. E.; Liu, J. A.; Rand, L.; Roy, S. *J. Visualized Exp.* **2014**, e51745.
(32) Ladd, C.; So, J. H.; Muth, J.; Dickey, M. D. *Adv. Mater.* **2013**, *25*, 5081−5085.
(33) Parekh, D. P.; Ladd, C.; Panich, L.; Moussa, K.; Dickey, M. D. *Lab Chip* **2016**, *16*, 1812−1820.
(34) Miller, A. R.; Davis, G. L.; Oden, Z. M.; Razavi, M. R.; Fateh, A.; Ghazanfari, M.; Abdolrahimi, F.; Poorazar, S.; Sakhaie, F.; Olsen, R. J.; Bahrmand, A. R.; Pierce, M. C.; Graviss, E. A.; Richards-Kortum, R. *PLoS One* **2010**, *5*, e11890.
(35) Hasan, M. M.; Alam, M. W.; Wahid, K. A.; Miah, S.; Lukong, K. E. *PLoS One* **2016**, *11*, e0167863.
(36) Ozcan, A. *Lab Chip* **2014**, *14*, 3187.
(37) Fu, E.; Liang, T.; Houghtaling, J.; Ramachandran, S.; Ramsey, S. A.; Lutz, B.; Yager, P. *Anal. Chem.* **2011**, *83*, 7941−7946.
(38) Zhou, G.; Bergeron, S.; Juncker, D. *J. Proteome Res.* **2015**, *14*, 1872−1879.

DOI: 10.1021/acs.analchem.7b01315
Anal. Chem. 2017, 89, 6846−6853